International Journal of Mechanical, Industrial and Aerospace Sciences
ISSN: 2517-9950
Vol:14, No:10, 2020

Numerical Simulation on Deformation Behaviour of Additively Manufactured AlSi10Mg Alloy

Racholsan Raj Nirmal, B. S. V. Patnaik, R. Jayaganthan

Abstract**—**The deformation behaviour of additively manufactured AlSi10Mg alloy under low strains, high strain rates and elevated temperature conditions is essential to analyse and predict its response against dynamic loading such as impact and thermomechanical fatigue. The constitutive relation of Johnson-Cook is used to capture the strain rate sensitivity and thermal softening effect in AlSi10Mg alloy. Johnson-Cook failure model is widely used for exploring damage mechanics and predicting the fracture in many materials. In this present work, Johnson-Cook material and damage model parameters for additively manufactured AlSi10Mg alloy have been determined numerically from four types of uniaxial tensile test. Three different uniaxial tensile tests with dynamic strain rates (0.1, 1, 10, 50, and 100 s^{-1}) and elevated temperature tensile test with three different temperature conditions (450 K, 500 K and 550 K) were performed on 3D printed AlSi10Mg alloy in ABAQUS/Explicit. Hexahedral elements are used to discretize tensile specimens and fracture energy value of 43.6 kN/m was used for damage initiation. Levenberg Marquardt optimization method was used for the evaluation of Johnson-Cook model parameters. It was observed that additively manufactured AlSi10Mg alloy has shown relatively higher strain rate sensitivity and lower thermal stability as compared to the other Al alloys.

Keywords**—**ABAQUS, additive manufacturing, AlSi10Mg, Johnson-Cook model.

I. Introduction

THE evolution of AlSi10Mg from additive manufacturing technology has been growing very quickly because of its super mechanical properties compared to production from conventional casting route. The additive manufacturing route controls the laser processing parameters and build parameters which enables to achieve unique microstructural features such as grain morphology, textures, reduced porosity content and residual stresses.

Li et al. [1] have fabricated additively manufactured AlSi10Mg alloy from selective laser melting (SLM-AM) to investigate its microstructure evolution and fracture behaviour. They have compared the values of yield stress and fracture stress in different post-processing techniques. Yield stress and fracture stress have higher values in as-built condition for vertical component (300 MPa and 455 MPa respectively) compared to other post-processes. Similarly, Raja et al. [2], [3] have investigated the tensile properties of AlSi10Mg alloy fabricated by SLM under the influence of working environments (Argon and Nitrogen) and built orientation. They have concluded that the tensile properties of AlSi10Mg are influenced more by the built orientation (vertical component has more strength than horizontal component) compared to working environment. Hitzler et al. [4] reported fracture toughness value of selective laser melted AlSi10Mg alloy from various fracture toughness tests and it lie in the range from 40 to 60 MPa$\sqrt{m}$.

Johnson-Cook model is the most frequently used model to simulate the impact phenomenon of metallic materials by using Finite element method (FEM). It only requires a few tensile tests to evaluate five material model parameters of Johnson-Cook model. Banerjee et al. [5] have reported a methodical approach to obtain the Johnson-Cook Material and damage model for armour steel. Determination of Johnson-Cook model parameters using Levenberg–Marquardt search algorithm and influence of strain rate sensitivity on flow behaviour of materials are discussed by [6] and [7] respectively.

This paper deals with the optimization of Johnson-Cook material and damage model parameters for additively manufactured AlSi10Mg alloy from various tensile tests at room temperature and elevated temperature and dynamic tests over wide range of strain rates.

II. Tensile Testing Simulation

Li et al. [1] obtained the engineering stress and engineering strain values for additively manufactured AlSi10Mg alloy upon different post-processing techniques through experiments, which is illustrated in Fig. 1. In the present work, engineering stress and engineering strain values of the as-built condition are used to perform FE tensile simulations as shown in Table I.

Gupta et al. [8] obtained the Johnson-Cook material model parameters for Aluminium plates from tensile tests on specimen geometries, as shown in Fig. 2. Similarly, the tensile test simulations are performed on specimens (Fig. 2) to obtain Johnson-Cook material model parameters of 3D printed AlSi10Mg alloy. FEM tensile test simulations are conducted with values shown in Table I on the tensile test specimens illustrated in Fig. 2 (a) to obtain material model parameters ‘A’, ‘B’ and ‘n’. Dynamic test simulations are performed on cylindrical specimen, which is depicted in Fig. 2 (b) for the determination of material model parameter ‘C’.

In the present work, isotropic hardening plasticity model is

Racholsan Raj Nirmal is with Department of Applied Mechanics and Department of Engineering Design, Indian Institute of Technology, Madras, Tamilnadu, India (phone: 8109653767; e-mail: racholsanraj@gmail.com).

B.S.V. Patnaik is with Department of Applied Mechanics, Indian Institute of Technology Madras, Tamilnadu, India (phone: 044-2257-4068, fax: 044-2257-4068; e-mail: bsvp@iitm.ac.in).

C. R. Jayaganthan is with Department of Engineering Design, Indian Institute of Technology Madras, Tamilnadu, India (phone: 044-2257-4735, fax: 044-2257-4735, e-mail: edjay@iitm.ac.in).

used for plastic deformation in FE simulation.

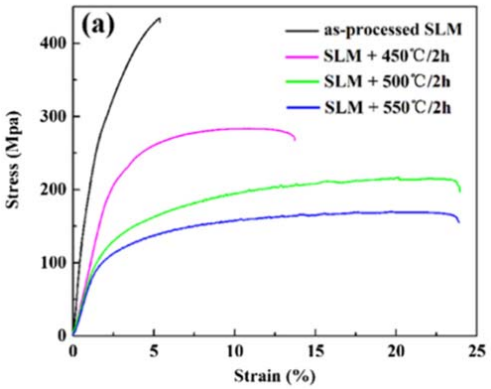

Fig. 1 Engineering stress versus engineering strain curves of SLM AlSi10Mg specimens after various heat-treatment processes taken from [1]

TABLE I
TRUE STRESS AND PLASTIC STRAIN VALUES FOR SIMPLE AND NOTCHED SPECIMENS

True Stress (Pa)	Plastic strain
331171900	0.024985
344179000	0.027031
360500000	0.029559
375051600	0.032661
394830300	0.035657
417842000	0.041142
449785200	0.049647
458751000	0.053162

The density, Young's modulus and Poisson's ratio are provided in the material feature of ABAQUS as 2700 kg/m^3, 75 GPa and 0.3 respectively. Kinematic coupling is used to restrict the movement on one side of the specimen as a constraint. The general static step is provided with a total time period of 1 second and an initial increment of 0.01 second. The hexahedral element (C38DR element) is used for the meshing of a tensile specimen with 20216 nodes and 17516 elements, as shown in Fig.3a. The FE simulations are performed over different strain rates (10^{-1} ,1,10,50 and 100 s^{-1}) at room temperature (298 K).

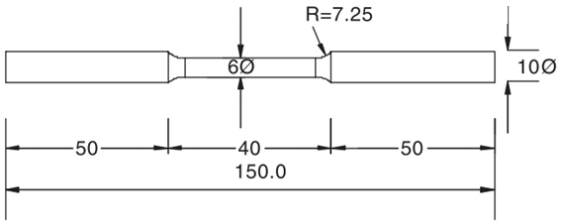

(a)

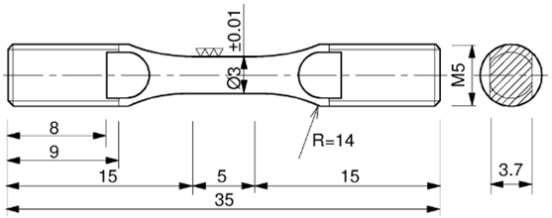

(b)

Fig. 2 Geometry of specimen for (a) FE tensile test simulations [8] (b) Tensile test simulations at dynamic strain rate [9] (all dimensions are in mm)

FE simulations are performed on the cylindrical specimen (Fig. 2 (a)) with different temperatures (450 K, 500 K and 550 K) to obtain the effect of elevated temperature on tensile specimens.

The tensile test specimen shown in Fig. 3 (b) represents the plastic deformation at 1 s^{-1} strain rate. Similarly, the tensile test simulations are performed for the other two strain rates (10 and 0.1 s^{-1}). Different engineering stress and strain values are obtained for three strain rates (10,1and 0.1 s^{-1}) during the plastic deformation. These values are used as inputs to calculate true plastic stress and strain values for determination of Johnson-Cook material model parameters.

III. DETERMINATION OF JOHNSON-COOK MATERIAL MODEL PARAMETERS

Johnson-Cook material model expresses the equivalent plastic stress as a function of plastic strain, strain rate, and temperature [10], as given in (1):

$$\sigma_{eq} = \left[A + B\varepsilon_p^n\right][1 + Cln(\dot{\varepsilon}^*)][1 - T^{*m}] \quad (1)$$

where, A, B, C, n, and m are material model constants, ϵ_p is accumulated plastic strain, $\dot{\varepsilon}^* = \frac{\dot{\varepsilon_p}}{\dot{\varepsilon_0}}$ is a dimensionless strain rate, $\dot{\varepsilon_0}$ is reference strain rate and $T^* = \frac{T-T_0}{T_m-T_0}$. These five material model parameters are evaluated by FEM tensile test simulation discussed in the following subsections (*A-C*).

A. Material Model Constants 'B' and 'n'

When the deformation temperature is at reference temperature $T = T_{ref} = 298K$ and the deformation strain rate is $\dot{\varepsilon}^* = \dot{\varepsilon}_f^* = 1s^{-1}$, then Johnson-Cook Material model equation (1) is modified as:

$$\sigma_{eq} = [A + B\varepsilon^n] \quad (2)$$

$$\sigma_{eq} - A = B\epsilon^n \quad (3)$$

Rearranging and taking the natural logarithm on both sides,

$$\ln(\sigma - A) = nln\epsilon + lnB \quad (4)$$

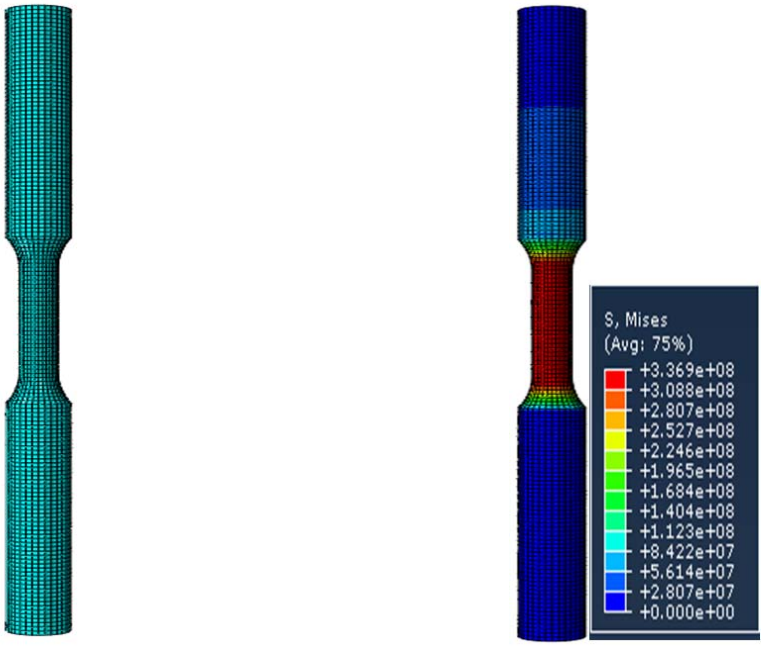

(a) (b)

Fig. 3 (a) Mesh of the tensile test specimen (b) FE simulation of the tensile test specimen

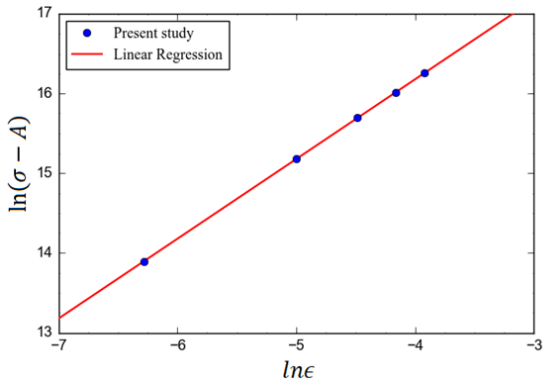

Fig. 4 True Plastic stress versus True Plastic strain for additively manufactured AlSi10Mg alloy

The value of 'A', which is the yield stress of the material under reference conditions, found to be 331.17 MPa. Equivalent plastic stress and equivalent plastic strain values are substituted in (4), which describes linear relationship between logarithmic values of equivalent plastic stress (σ_{eq}) and equivalent plastic strain (ε) depicted in Fig. 4. 99.46% data points are closer to the regression line in the figure. Five distinct data points are used for curve fitting optimization by least square method. The slope of the line represents value of 'n'. The first order regression analysis of the regression curve shown in Fig. 4 provides the material model parameters B and n:

A = 331.17 MPa, B = 579.647 MPa, and n = 0.99

B. Material Constants 'C'

When the deformation temperature is $T = T_{ref} = 298K$ in (1), Johnson-Cook material model can be modified as:

$$\sigma_{eq} = [A + B\varepsilon^n][1 + Cln\dot{\varepsilon}^*] \quad (5)$$

$$\frac{\sigma_{eq}}{[A+B\varepsilon^n]} = [1 + Cln\dot{\varepsilon}^*] \quad (6)$$

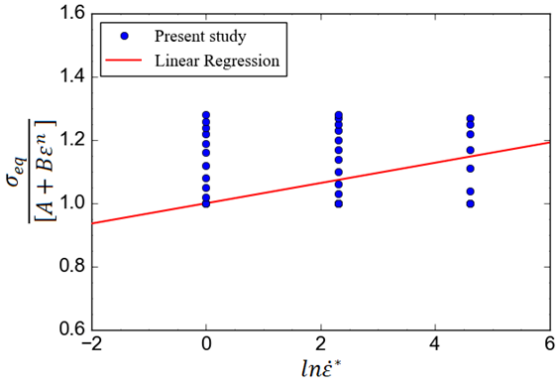

Fig 5 Curve fitting for 'C' value for additively manufactured AlSi10Mg alloy

A, B, and n values are used as input in (6) from the already obtained result. Tensile test simulation is performed for three different strain rates (10,1 and 0.1 s^{-1}) on the specimen shown in Fig. 2 (b) to get equivalent flow stress at those strain rates to plot the graph between $\frac{\sigma_{eq}}{[A+B\varepsilon^n]}$ and $Cln\dot{\varepsilon}^*$. In Fig. 5, $\frac{\sigma_{eq}}{[A+B\varepsilon^n]}$ represents ordinate and natural logarithm of strain rates ($ln\dot{\varepsilon}^*$)

represents abscissa.

In Fig .5, $\frac{\sigma_{eq}}{[A+B\varepsilon^n]}$ versus $ln\dot{\varepsilon}^*$ is drawn to curve fit, where the value of intercept on the ordinate is 1. Slope of the line represents material model parameter C, which is determined to be 0.032. Strain rate sensitivity has higher values for additively manufactured aluminium alloy compared to the cast Aluminium alloys reported by [11] and [12].

C. Material Model Constants 'm'

When the deformation strain rate is $\dot{\varepsilon} = \dot{\varepsilon}_{ref} = 1s^{-1}$ in (1), then Johnson-Cook material model equation can be written as:

$$\sigma_{eq} = [A + B\varepsilon^n][1 - T^{*m}] \quad (7)$$

$$1 - \frac{\sigma_{eq}}{[A+B\varepsilon^n]} = T^{*m} \quad (8)$$

$$ln\left[1 - \frac{\sigma_{eq}}{[A+B\varepsilon^n]}\right] = mlnT^* \quad (9)$$

Substituting the material constants A, B and n values in (9) and using a first-order regression model for fitting data points, material model parameter 'm' is evaluated from the slope of the fitted curve between $ln\left[1 - \frac{\sigma_{eq}}{[A+B\varepsilon^n]}\right]$ versus lnT^*.

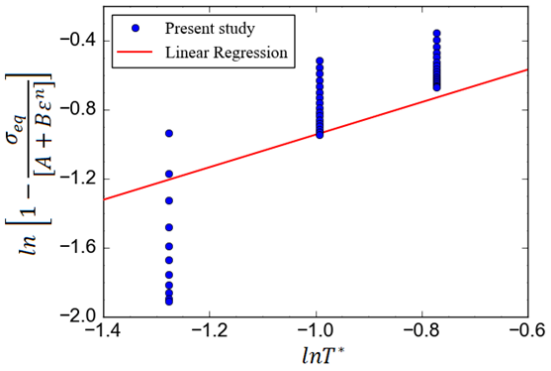

Fig. 6 Determination of material model constant 'm' for 3D printed AlSi10Mg alloy

Tensile test simulations are performed on the specimen shown in Fig. 2 (b) to simulate the temperature effect in 3D printed AlSi10Mg alloy. Coefficient of thermal expansion value of $2\times10^{-5}\ K^{-1}$ and thermal conductivity of 190 W/mK are used in the simulation which is taken from the thermal expansion coefficient of additively manufactured AlSi10Mg alloy reported by [13]. Six different data points are obtained for each temperature from the flow stress values of three different temperatures (450 K, 500 K and 550 K) for optimization purposes. The slope of the line in (7) represents value of 'm'. The value of material model parameter 'm' is determined to be 0.945 from Fig. 6. Additively manufactured AlSi10Mg alloy is less thermally stable compared to the 2024 Aluminium alloy as reported by [14] and [15]

IV. Tensile Testing Simulation of Notched Specimen

Johnson-Cook damage parameters are determined from tensile test simulations performed on specimens shown in Fig. 8. The geometry of specimens creates different stress triaxiality ratios, which are generated from different thicknesses and notch radii. Gupta et al. [8] have used this specimen (Fig. 7) to obtain the damage parameters of the Johnson-Cook model for aluminium plates. Similarly, FE tensile test simulations are performed on these specimens with different notch radii and ductile damage as failure criterion.

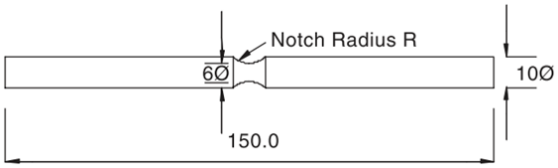

Fig. 7 Geometry of Notched specimen

The specimen in Fig. 7 represents tensile test notched specimen with double U-notch on their working length for simulations. Notched specimens have different width and notch radii to ensure that the triaxiality ratio is higher in the first and second specimen compared to the third specimen in Fig. 8. The study by Niu et al. [16] on doubly U-notched specimens has shown that the decreasing order of notch radii results in the decreasing tendency of rupture plastic strain with decreasing stress triaxiality ratio. Three different notch radii (2, 3 and 4 mm) were used for FE simulations (Fig. 8 (b)) to generate different stress triaxiality ratios and an artificial notch was produced for the initiation of damage in case of smooth specimen as shown in Fig. 2 (a).

The material properties used in tensile test simulation of the simple specimen are also used for the simulations of these notched specimens to evaluate three damage parameters D_1, D_2 and D_3. Dynamic test simulations performed on the specimen shown in Fig. 2 (b) are simulated for three different low strain rates (10,50 and 100 s^{-1}). Ductile damage model is used for the plastic deformation. Non-linear geometrical (Nlgeom) feature in ABAQUS is checked for the large displacements. Dynamic explicit simulations are performed on these specimens with kinematic coupling as a constraint on one side of the specimens.

The images of the deformed state of un-notched and notched specimens are presented in Fig. 8. The un-notched specimen displays the stress effect on the working length to be less compared to the notched specimen. The rupture strain is more in notched specimen with 4 mm notch radii compared to the notched specimen with 2 mm and 3 mm notch radii, which proves that with the increase of stress triaxiality ratio, the rupture strain increases. To measure the strain rate sensitivity effect on fracture strain of specimen dynamic tensile test simulations are performed at three different strain rates ($10\ s^{-1}, 50\ s^{-1}$ and $100\ s^{-1}$) on the specimen shown in Fig. 2 (b). The tensile test simulations are also performed at three different temperatures conditions (450K, 500K and 550K) on

the specimen shown in Fig. 2 (a) to evaluate the effect of temperature on fracture strain of specimen.

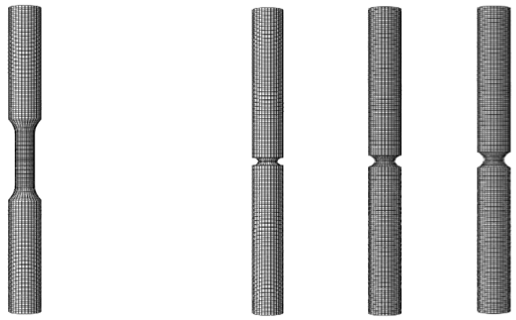

Fig. 8 Tensile testing simulation of (a) un-notched specimen, (b) notched specimens with 2, 3 and 4 mm notch radii

Following Ductile damage model values are used in the numerical simulations: Fracture strain (ε_f) = 0.05301, Stress triaxiality = 0.33 and Strain rate = 1 s^{-1}

V. Determination of Johnson-Cook Damage Model Parameters

The model by Johnson & Cook proposes that true plastic fracture strain ε_f depends on stress triaxiality, strain rate, and temperature and can be expressed as:

$$\varepsilon_f = [D_1 + D_2 exp\,(D_3\sigma^*)\,][1 + D_4 ln\,(\dot{\varepsilon}^*)\,][1 + D_5 T^*] \quad (10)$$

where D_1 to D_5 are damage constants, $\sigma^* = \frac{\sigma_m}{\sigma_{eq}}$ is the stress triaxiality ratio and σ_m is mean stress or hydrostatic stress. σ_{eq} is obtained from Johnson-Cook constitutive relation for original (undamaged) material

$$\sigma_{eq} = \frac{\frac{\sigma_1+\sigma_2+\sigma_3}{3}}{\sqrt{0.5\times[(\sigma_1^2-\sigma_2^2)+(\sigma_2^2-\sigma_3^2)+(\sigma_3^2-\sigma_1^2)]}} \quad (11)$$

where σ_1, σ_2 & σ_3 are principal stresses in x, y & z-direction.

As reported by Bao et al., the formula for stress triaxiality ratio is used to evaluate the stress triaxiality ratios of un-notched specimen and notched specimens [10], [17]:

$$\eta = \frac{1}{3} + \sqrt{2}\ln\left[1 + \frac{t}{4R}\right] \quad (12)$$

where η = stress triaxiality ratio, t = thickness of notched part, R = Radius of notched area.

TABLE II
Stress Triaxiality Ratios for Different Specimens

Specimen	Stress triaxiality ratio
Un-notched specimen	0.33
Notched specimen 1	1.123
Notched specimen 2	0.9067
Notched specimen 3	0.784

From (12), the stress triaxiality ratios of un-notched specimen and notched specimen 1 and 2 are evaluated, which is shown in Table II. These values are used in the evaluation of damage parameters of Johnson Cook model for additively manufactured AlSi10Mg alloy.

A. Damage Parameters (D_1, D_2 and D_3)

Johnson-Cook damage model in (10) can be written in the form of (13) at reference strain rate $(\dot{\varepsilon}^* = \dot{\varepsilon}_f^* = 1s^{-1})$ and temperature $(T = T_{ref} = 298K)$:

$$\varepsilon_f = D_1 + D_2\, exp(D_3\sigma^*) \quad (13)$$

All four specimens are tested at reference strain rate and reference temperature.

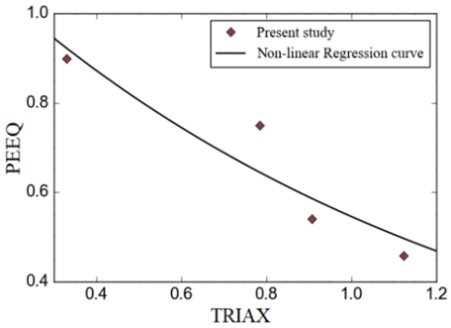

Fig. 9 PEEQ versus TRIAX to evaluate D_1, D_2 and D_3

The values of equivalent plastic strain (ε_f) and triaxiality ratio (σ^*) are substituted in (13). In Fig. 9, the plot is drawn between TRIAX against PEEQ, and the regression curve is plotted to determine the coefficients specified in (10).

The following damage parameters are obtained from the Levenberg Marquardt optimization as shown in Fig. 8: D_1= 0.04704, D_2 = 1.155 & D_3= -0.841

B. Damage Parameter D_4

Rearranging the Johnson Cook damage model in (10), the value of D_4 at reference temperature 298 K is obtained using (15):

$$\varepsilon_f = [D_1 + D_2 exp\,(D_3\sigma^*)\,][1 + D_4\, ln\,(\dot{\varepsilon}^*)\,] \quad (14)$$

$$\frac{\varepsilon_f}{[D_1+D_2\, exp\,(D_3\,\sigma^*)]} = [1 + D_4\, ln\,(\dot{\varepsilon}^*)\,] \quad (15)$$

D_1, D_2 & D_3 values from Section V *A* are substituted in (15), and then tensile test simulations for equivalent plastic strain at three different plastic strain rates ($10\ s^{-1}, 50\ s^{-1}$ & $100\ s^{-1}$) were performed on the specimen shown in Fig. 2 (b).

In Fig. 10, the natural logarithm of three different strain rates (10,50 & 100 s^{-1}) represents abscissa (as reference strain rate = 1) and $\frac{\varepsilon_f}{[D_1+D_2 exp\,(D_3\sigma^*)\,]}$ represents ordinate. The first order regression curve is drawn with ordinate value as 1. The slope of line in (15) provides Johnson-Cook damage parameter D_4. From the curve fitting according to Levenberg

Marquardt optimization, damage parameter D_4 is evaluated as -0.042.

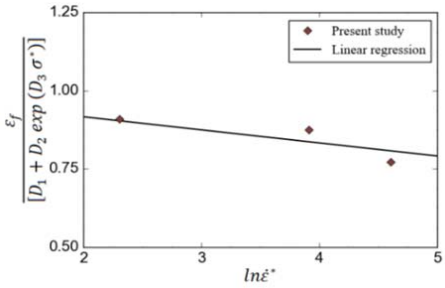

Fig. 10 Curve fitting for D_4 value

C. Damage Parameter D_5

Johnson-Cook damage model equation is rearranged to obtain D_5 value for a notched specimen using (10) at reference strain rate ($\dot{\varepsilon}^*$= 1).

$$\varepsilon_f = [D_1 + D_2 exp\,(D_3\sigma^*)\,][1 + D_5 T^*] \quad (16)$$

$$\frac{\varepsilon_f}{[D_1 + D_2 exp\,(D_3\sigma^*)\,]} = 1 + D_5 T^* \quad (17)$$

Simulations are performed at three different temperature conditions (450 K, 500 K and 550 K) in ABAQUS. T^* values for these three different temperatures are 0.28, 0.37 and 0.46, respectively. Different effective plastic strain values (ε_f) at T^* values are substituted in (17) along with the values of damage parameters D_1, D_2, and D_3. The effect of temperature change on these notched specimens was negligible and therefore it is accounted to be zero. Table III provides the numerically obtained material and damage model parameters of additively manufactured AlSi10Mg alloy.

TABLE III
NUMERICALLY OBTAINED JOHNSON-COOK MATERIAL AND DAMAGE MODEL PARAMETER FOR ADDITIVELY MANUFACTURED ALSI10MG ALLOY

Material model parameters		Damage model parameters	
Yield stress, A	331.17 MPa	D_1	0.04704
Strain hardening parameter, B	579.647 MPa	D_2	1.155
Strain hardening exponent, n	0.99	D_3	-0.841
Strain rate sensitivity parameter, C	0.032	D_4	-0.042
Temperature exponent, m	0.945	D_5	0

VI. CONCLUSION

The purpose of the numerical simulation described in this work is to develop a Johnson-Cook material and damage model for additively manufactured AlSi10Mg alloy. Tensile test simulations on simple and notched specimens at room temperature (298 K) and elevated temperature (450 K, 500 K and 550 K), dynamic test simulations were performed for wide strain range (0.1 to 100 s^{-1}) to evaluate Johnson-Cook material and damage model parameters for additively manufactured AlSi10Mg alloy.

ACKNOWLEDGMENT

The authors would like to gratefully acknowledge the Department of Engineering Design, Indian Institute of Technology, Madras for providing the tools required for performing simulations and evaluation.

REFERENCES

[1] W. Li *et al.*, "Materials Science & Engineering A Effect of heat treatment on AlSi10Mg alloy fabricated by selective laser melting : Microstructure evolution, mechanical properties and fracture mechanism," *Mater. Sci. Eng. A*, vol. 663, pp. 116–125, 2016, doi: 10.1016/j.msea.2016.03.088.

[2] S. R. Ch, A. Raja, R. Jayaganthan, N. J. Vasa, and M. Raghunandan, "Study on the fatigue behaviour of selective laser melted AlSi10Mg alloy," *Mater. Sci. Eng. A*, vol. 781, no. March, p. 139180, 2020, doi: 10.1016/j.msea.2020.139180.

[3] S. R. Ch, A. Raja, P. Nadig, R. Jayaganthan, and N. J. Vasa, "Influence of working environment and built orientation on the tensile properties of selective laser melted AlSi10Mg alloy," *Mater. Sci. Eng. A*, vol. 750, no. October 2018, pp. 141–151, 2019, doi: 10.1016/j.msea.2019.01.103.

[4] L. Hitzler *et al.*, "Fracture toughness of selective laser melted AlSi10Mg," *Proc. Inst. Mech. Eng. Part L J. Mater. Des. Appl.*, vol. 233, no. 4, pp. 615–621, 2019, doi: 10.1177/1464420716687337.

[5] A. Banerjee, S. Dhar, S. Acharyya, D. Datta, and N. Nayak, "Determination of Johnson cook material and failure model constants and numerical modelling of Charpy impact test of armour steel," *Mater. Sci. Eng. A*, vol. 640, pp. 200–209, 2015, doi: 10.1016/j.msea.2015.05.073.

[6] A. Shrot and M. Bäker, "Determination of Johnson-Cook parameters from machining simulations," *Comput. Mater. Sci.*, vol. 52, no. 1, pp. 298–304, 2012, doi: 10.1016/j.commatsci.2011.07.035.

[7] L. Gambirasio and E. Rizzi, "An enhanced Johnson-Cook strength model for splitting strain rate and temperature effects on lower yield stress and plastic flow," *Comput. Mater. Sci.*, vol. 113, pp. 231–265, 2016, doi: 10.1016/j.commatsci.2015.11.034.

[8] N. K. Gupta, M. A. Iqbal, and G. S. Sekhon, "Experimental and numerical studies on the behavior of thin aluminum plates subjected to impact by blunt- and hemispherical-nosed projectiles," *Int. J. Impact Eng.*, vol. 32, no. 12, pp. 1921–1944, 2006, doi: 10.1016/j.ijimpeng.2005.06.007.

[9] T. Borvik, O. S. Hopperstad, T. Berstad, and M. Langseth, "A computational model of viscoplasticity and ductile damage for impact and penetration," *Eur. J. Mech. A/Solids*, vol. 20, no. 5, pp. 685–712, 2001, doi: 10.1016/S0997-7538(01)01157-3.

[10] M. Murugesan and D. W. Jung, "Johnson cook material and failure model parameters estimation of AISI-1045 medium carbon steel for metal forming applications," *Materials (Basel).*, vol. 12, no. 4, 2019, doi: 10.3390/ma12040609.

[11] S. Gupta, S. Abotula, and A. Shukla, "Determination of Johnson-Cook Parameters for Cast Aluminum Alloys," vol. 136, no. July, pp. 1–5, 2014, doi: 10.1115/1.4027793.

[12] K. Senthil, B. Arindam, M. A. Iqbal, and N. K. Gupta, "Ballistic Response of 2024 Aluminium Plates Against Blunt Nose Projectiles," *Procedia Eng.*, vol. 173, pp. 363–368, 2017, doi: 10.1016/j.proeng.2016.12.030.

[13] R. Gumbleton, J. A. Cuenca, G. M. Klemencic, N. Jones, and A. Porch, "Evaluating the coefficient of thermal expansion of additive manufactured AlSi10Mg using microwave techniques," *Addit. Manuf.*, vol. 30, no. September, p. 100841, 2019, doi: 10.1016/j.addma.2019.100841.

[14] P. Sharma, P. Chandel, P. Mahajan, and M. Singh, "Quasi-Brittle Fracture of Aluminium Alloy 2014 under Ballistic Impact," *Procedia Eng.*, vol. 173, pp. 206–213, 2017, doi: 10.1016/j.proeng.2016.12.059.

[15] M. A. Iqbal, K. Senthil, V. Madhu, and N. K. Gupta, "Oblique impact on single, layered and spaced mild steel targets by 7.62 AP projectiles," *Int. J. Impact Eng.*, vol. 110, pp. 26–38, 2017, doi: 10.1016/j.ijimpeng.2017.04.011.

[16] L. Bin Niu, H. Takaku, and M. Kobayashi, "Tensile fracture behaviors in double-notched thin plates of a ductile steel," *ISIJ Int.*, vol. 45, no. 2, pp. 281–287, 2005, doi: 10.2355/isijinternational.45.281.

[17] Y. Bai, X. Teng, and T. Wierzbicki, "On the application of stress triaxiality formula for plane strain fracture testing," *J. Eng. Mater. Technol. Trans. ASME*, vol. 131, no. 2, pp. 0210021–02100210, 2009, doi: 10.1115/1.3078390.